

RESEARCH

Open Access



A novel senotherapeutic strategy with azithromycin for preventing endometriosis progression

Reina Sonehara¹, Tomoko Nakamura^{1*}, Takehiko Takeda², Satoshi Kaseki¹, Tomomi Seki¹, Hideaki Tanaka², Atsushi Yabuki¹, Natsuki Miyake¹, Ayako Muraoka², Satoko Osuka¹, Akira Iwase³ and Hiroaki Kajiyama¹

Abstract

Background Endometriosis is an estrogen-dependent chronic inflammatory disease, however the mechanisms underlying inflammation remain unclear. Non-hormonal drugs that can prevent endometriosis progression and resolve endometriotic infertility are urgently required. We thus focused on cellular senescence as a novel feature of endometriosis. Senescent cells cause chronic inflammation via the senescence-associated secretory phenotype (SASP) factor. It has been reported the effects of senolysis for various diseases in recent years. The aim of this study was to validate the involvement of cellular senescence in endometriosis and as the effects of senolytic drug to develop a novel non-hormonal therapeutic strategy for endometriosis.

Methods The senescence markers were assessed by morphological features and semiquantitative immunofluorescence staining (senescence-associated β -galactosidase [SA- β -Gal], the cyclin-dependent kinase inhibitor 2 A locus [p16^{INK4a}], and laminB1) to compare among cell types (normal endometrial stromal cells [nESCs], endometrial stromal cells with endometriosis [eESCs], and ovarian endometriosis [OE] cyst-derived stromal cells [CSCs]). Expression of SASP markers was examined in cell culture supernatants using a cytokine array. In addition, the effects of senolytic drugs (azithromycin [AZM] and navitoclax [ABT263]) on endometriosis were evaluated in vitro and in vivo. The in vivo study used the endometriosis mice model.

Results CSCs exhibited stronger senescence markers. Semi-quantitative SA- β -Gal and p16^{INK4a} staining intensities were significantly increased, and that of LaminB1 was decreased in CSCs compared to those in nESCs and eESCs (SA- β -Gal, $P < 0.001$; p16^{INK4a}, $P < 0.05$; LaminB1, $P < 0.05$). Cytokine array analysis revealed elevated SASP-related cytokine levels, including interleukin-6 (IL-6), in CSC supernatants compared to those in nESCs. AZM and ABT263 reduced the viable fraction in CSCs (AZM: $P < 0.001$, ABT263: $P < 0.01$). Furthermore, AZM suppressed IL-6 expression in CSC culture supernatants ($P < 0.05$). In murine model, AZM administration reduced endometriotic lesion volume compared to that in vehicle ($P < 0.05$). Proliferative activity, IL-6 expression levels, and fibrosis within endometriotic lesions also decreased (Ki67, $P < 0.01$; IL-6, $P < 0.001$; fibrosis, $P < 0.001$).

*Correspondence:
Tomoko Nakamura
yamaguchi.tomoko.t2@f.mail.nagoya-u.ac.jp

Full list of author information is available at the end of the article



© The Author(s) 2025. **Open Access** This article is licensed under a Creative Commons Attribution-NonCommercial-NoDerivatives 4.0 International License, which permits any non-commercial use, sharing, distribution and reproduction in any medium or format, as long as you give appropriate credit to the original author(s) and the source, provide a link to the Creative Commons licence, and indicate if you modified the licensed material. You do not have permission under this licence to share adapted material derived from this article or parts of it. The images or other third party material in this article are included in the article's Creative Commons licence, unless indicated otherwise in a credit line to the material. If material is not included in the article's Creative Commons licence and your intended use is not permitted by statutory regulation or exceeds the permitted use, you will need to obtain permission directly from the copyright holder. To view a copy of this licence, visit <http://creativecommons.org/licenses/by-nc-nd/4.0/>.

Conclusions Our findings show that cellular senescence is involved in the pathogenesis of endometriosis and that AZM may be useful for preventing endometriosis progression by suppressing the secretion of IL-6 as a SASP.

Keywords Endometriosis, Cellular senescence, SASP, IL-6, Senotherapy, Azithromycin

Introduction

Endometriosis is a chronic inflammatory disease in which ectopic endometrium engrafts and progresses, which exacerbates in an estrogen-dependent manner [1]. It affects approximately 10% of women of reproductive age and up to 50% of women with infertility [1]. Ovarian endometriosis (OE) is the most common type of endometriosis and is one of the main causes of menstrual pain and infertility [1]. Existing pharmacotherapies for endometriosis suppress follicle development and ovulation, thus preventing the patient from conceiving [1]. Therefore, non-hormonal drugs that can prevent endometriosis progression and contribute to resolving endometriotic infertility are urgently required [1].

Cellular senescence is a state of irreversible cell cycle arrest [2, 3]. Despite growth arrest, senescent cells display metabolic activity and secrete factors, including inflammatory cytokines, chemokines, growth factors, and matrix metalloproteinases, referred to as the senescence-associated secretory phenotype (SASP) [2–4]. There are two types of senescence; replicative senescence resulting from telomere shortening, and stress-induced premature senescence (SIPS) [2]. One of the major causes of SIPS is oxidative stress [5]. Senescent cells positively affect tissue homeostasis, normal development, wound healing, and carcinogenesis inhibition [2, 3, 6], while chronic SASP is implicated in various pathologies, including cancer, chronic inflammatory diseases, and age-related diseases [2, 3, 6]. Senescent cells impact their microenvironments in an autocrine and paracrine manner via SASP to promote senescence and inflammation [7–9]. Senotherapy is the pharmacotherapy to induce cell death (senolytics) or inhibit SASP (senomorphics) by targeting unique features of senescent cells [3, 10]. Senotherapy has attracted significant interest in treating cancer and chronic inflammatory diseases [10]. Efficacies of senotherapeutics, including anticancer agents, flavonoids, and antibiotics, have been reported, and a few are undergoing clinical trials [11].

Inflammation and oxidative stress are the key factors involved in the pathogenesis of endometriosis [12]. Inflammatory cytokines regulate endometrial proliferation, fibrosis, and infertility [13–18]. Murakami et al. reported the non-hormonal anti-inflammatory effects of reducing interleukin-1 beta (IL-1 β) expression and oxidative stress using the nucleotide-binding oligomerization domain, leucine-rich repeat, and pyrin domain-containing (NLRP) 3 inflammasome inhibitors in OE [19]. Oxidative stress is known to modulate cellular proliferation

in endometriosis, thereby leading to its development and progression [20]. However, the mechanisms underlying inflammation in endometriosis remain unclear. Although the involvement of cellular senescence in endometriosis has recently been reported [21–24], no studies have examined senotherapy in endometriosis. We thus focused on cellular senescence in endometriosis and senotherapeutics such as B-cell lymphoma-2 (BCL-2) protein inhibitor navitoclax (ABT263) and the antibiotic azithromycin (AZM), which have been reported to be highly specific against senescent fibroblasts [25, 26]. We hypothesized that senescent cells in endometriosis may cause chronic inflammation that exacerbates lesions through SASP, and that AZM or ABT263 may offer novel non-hormonal strategies for treating endometriosis.

In this study, we aimed to investigate the involvement of cellular senescence in endometriosis stroma and assess the effects of senotherapy to develop a novel non-hormonal therapeutic strategy for endometriosis.

Materials and methods

For in vitro experiments

Patients and sample collection

Patient samples were used for stromal cell isolation. All samples were obtained from the Nagoya University Hospital between July 2018 and November 2021. The Ethics Committee of Nagoya University Graduate School of Medicine (2017–0503) approved this study. Written informed consent was obtained from each patient who enrolled in this study. Samples were collected from 31 patients: OE samples from 22 patients, endometrial tissues with OE from 13 patients, and endometrial tissues without OE from 9 patients who diagnosed with mature cystic teratomas, leiomyomas, uterine anomalies, or cervical dysplasia, but no history or surgical findings of OE.

Primary human stromal cell isolation

Normal endometrial stromal cells (nESCs), endometrial stromal cells with OE (eESCs), and OE (chocolate cyst)-derived stromal cells (CSCs) were isolated from patient tissue and cultured as previously described [19]. Tissue were chopped in Dulbecco's modified Eagle's medium (DMEM; Nacalai Tesque, Kyoto, Japan) and incubated with collagenase solution (1 mg/mL; FUJIFILM Wako Pure Chemical Corporation Osaka, Japan) for 30 min at 37 °C. The cell suspension was filtered through 70 μ m filter membranes, followed by centrifugation to obtain a stromal cell pellet. nESCs, eESCs and CSCs were then resuspended in fresh DMEM containing 10% fetal bovine

serum (Cosmo Bio, Tokyo, Japan), 100 IU/mL penicillin, 100 mg/L streptomycin, and 25 mg/L amphotericin B. The next day, media containing unattached cells were transferred to a second dish before the media was removed and discarded. The cells were routinely maintained at 37 °C until they reached 90% confluence and were then seeded for experimental purposes, as details below. Depending on their growth, cells were used for sequential experiments in passages 2–7.

For detecting senescent cells

Senescence-associated- β -galactosidase (SA- β -Gal) staining

SA- β -Gal staining of cultured cells was performed to identify senescent cells. Staining was done according to a protocol modified from the previously described [27] using Senescence beta-Galactosidase Staining Kit (Cell Signaling Technology, Inc., Danvers, MA, USA). Cells were seeded into each well of a 6-well plate and allowed to adhere for 24 h. Adherent cells were washed once with phosphate-buffered saline (PBS) and then fixed in a solution containing 2% formaldehyde and 0.2% glutaraldehyde for 15 min at room temperature. After another two PBS washes, the cells were incubated in a staining solution (150 mM NaCl, 2 mM MgCl₂, 5 mM potassium ferricyanide, 5 mM potassium ferrocyanide, 2.45 mM [1 mg/mL] 5-bromo-4-chloro-3-indolyl- β -D-thiogalactopyranoside [X-Gal] in phosphate-citrate buffer, pH 6.0) at 37 °C without CO₂ overnight. The percentage of SA- β -Gal-positive cells was determined using an inverted microscope (Olympus IX51, Tokyo, Japan) by counting cells in five random fields of view at a magnification of 200 \times . Images were captured using a Canon 1100 digital camera (Tokyo, Japan). Staining intensity was quantified using ImageJ software (threshold 110).

SPiDER-Gal assay

SA- β -Gal activity was quantitated with a Cellular Senescence Plate Assay Kit using SPiDER- β Gal, a fluorogenic substrate for β -galactosidase (SG05, Dojindo, Kumamoto, Japan), following the manufacturer's instructions. The optimal cell numbers in each well were adjusted using a Cell Count Normalization Kit (C544, Dojindo, Kumamoto, Japan), following the manufacturer's instructions. Cells were lysed with Lysis Buffer for 10 min at room temperature, then incubated with SPiDER- β Gal working solution at 37 °C for 30 min. After adding a stop solution, using an excitation wavelength of 535 nm, emission at 580 nm was recorded using a multimode microplate reader (SpectraMax iD5, Molecular Devices, San Jose, CA, USA).

Immunocytochemistry

Cells were cultured on coverslips for 24 h, fixed in methanol for 2 min at room temperature, and permeabilized

with 0.5% Triton X-100 for 1 min. After blocking with 1% bovine serum albumin for 1 h at room temperature, cells were incubated with primary antibodies against P16^{INK4a} (ab108349, 1:100, Abcam, Cambridge, UK), LaminB1 (MA1-06103, 1:100, Thermo Fisher Scientific, Waltham, MA, USA), and IL-6 (MAB2061, Bio-Techne, MN, USA) or 2 h at room temperature. Cells were then incubated with goat anti-rabbit (Alexa Fluor[®] 568, 1:500, Thermo Fisher Scientific, Waltham, MA, USA, for anti-P16^{INK4a} antibody) or goat anti-mouse (Alexa Fluor[®] 488, 1:500, Thermo Fisher Scientific, Waltham, MA, USA, for anti-LaminB1 antibody and anti-IL-6 antibody) secondary antibodies for 1 h at room temperature. Nuclear staining was performed using 4',6-diamidino-2-phenylindole (4083, 1:1000; Cell Signaling Technology, Danvers, MA, USA). Visualization was performed using a confocal laser-scanning microscope (BZ9000, Keyence, Osaka, Japan).

For evaluating effects of senolytics

Cell viability assay

The effect of AZM and ABT263 on cell viability were determined using cell counting. Cells (1.0×10^5) were seeded into each well of a 6-well plate and allowed to adhere for 24 h. The cells were cultured in serum-free media for 24 h, followed by treatments with AZM (azithromycin, 50 μ M, PZ0007 Sigma Aldrich, St. Louis, MO, USA) for 72 h or ABT263 (navitoclax, 1 μ M, HY-10087, MedChemExpress, Monmouth Junction, NJ, USA) for 24 h. Concentrations of AZM and ABT263 were applied in accordance with previous reports [25, 26]. Finally, 1 mL of 0.25% trypsin was added to each well, and cells were incubated with it for 5 min at 37 °C. Detached cells were collected and centrifuged, and the number of viable cells was counted.

Cytokine analysis

nESCs and CSCs were treated for 72 h with 50 μ M AZM. Cytokines secreted by the cells were detected in conditioned medium using RayBiotech Human Cytokine Arrays C3 according to the manufacturer's instructions (RayBiotech Inc., Peachtree Corners, GA, USA). A LAS4000 CCD Imaging System (Fujifilm Co. Ltd., Tokyo, Japan) was used to detect proteins. The signal intensity of each spot, which represented the secreted cytokines, was evaluated by subtracting the background and normalizing to positive controls using ImageJ software.

Chemiluminescent enzyme immunoassay (CLEIA)

nESCs and CSCs were treated for 72 h with 50 μ M AZM or for 24 h with 1 μ M. Interleukin-6 (IL-6) concentrations in the culture supernatants were measured using the CLEIA method (FUJIREBIO, Tokyo, Japan) at an outsourced laboratory (H.U. Frontier, Inc., Tokyo, Japan).

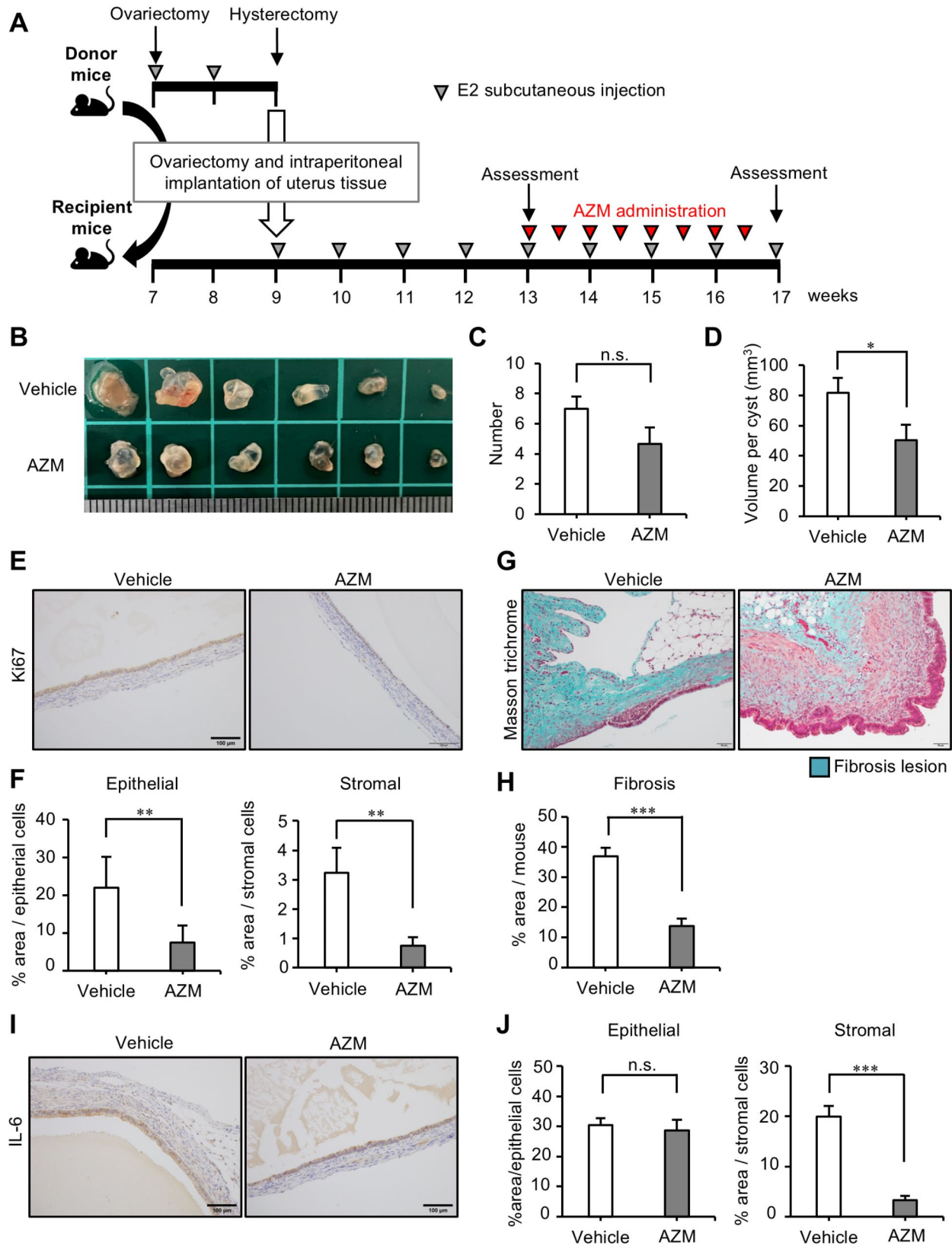


Fig. 1 (See legend on next page.)

(See figure on previous page.)

Fig. 1 AZM prevents endometriosis progression in murine models. **(A)** Our experimental protocol is shown. Four weeks after uterine tissue transplantation, recipient mice were treated with 50 mg/kg AZM twice weekly. **(B–D)** The numbers of endometriosis lesions were comparable in both groups, while volume per endometriosis lesion was reduced in the AZM group. **(E)** Representative Ki67 immunohistochemical images of endometriosis lesions. Scale bar: 100 μ m. **(F)** Percentages of Ki67-positive cells in endometriosis lesions decreased in the AZM group in both epithelial and stromal cells. **(G)** Representative Masson trichrome staining analysis results of endometriosis lesions. Scale bar: 50 μ m. **(H)** Fibrotic lesions within endometriosis cysts were significantly reduced in the AZM group. **(I)** Representative images of IL-6 immunohistochemistry in endometriosis lesions. **(J)** IL-6-positive areas in stromal cell lesions were significantly decreased in the AZM group ($n=6$ in each group). AZM, azithromycin. Data are shown as means \pm SEM. Data were analyzed by the Student's *t* test. * $P < 0.05$; ** $P < 0.01$; *** $P < 0.001$; n.s., not significant

For in vivo experiments

Animal experiment

A murine endometriosis model was used as previously described [28]. The experimental protocol is summarized in Fig. 1A. Female mice (6-week-old, BALB/c) were purchased from Japan SLC (Shizuoka, Japan). All animal experiments were approved by the Animal Experimental Committee of the Nagoya University Graduate School of Medicine (M230117-002 and M230297-002). Before starting the experiments, animals were acclimated for 7 days at 23–25 °C with a 12 h/12 h dark/light cycle and were given standard chow (CE-2; CLEA Japan, Tokyo, Japan) and water. Cage linings were changed every week.

Donor mice were ovariectomized and injected subcutaneously with 17 β -estradiol (E2, 100 μ g/kg per mouse once a week; Fuji Pharma, Tokyo, Japan) in olive oil. After two weeks, donor uteri were removed after euthanasia. The uteri were slit longitudinally with a linear incision and minced using fine scissors. Twelve recipient mice (9-week-old) were anesthetized with isoflurane and ovariectomized. The minced donor uterine tissue, equivalent to half of a uterus dispersed in 500 μ L saline, was injected into the peritoneal cavity. Recipient mice were injected subcutaneously with E2 (100 μ g/kg) in olive oil once a week for eight weeks until the end of the experiment (17-week-old), when autopsies were performed.

Four weeks after transplantation, 12 recipient mice were divided into 2 groups, AZM or vehicle group. Six mice were treated with AZM (50 mg/kg, A9834, LKT, St. Paul, MN, USA) and the other 6 mice were treated with 0.5% carboxymethyl cellulose (CMC, C4888, Sigma Aldrich, Saint Louis, MO, USA) orally twice a week. The first dose of AZM was administered the day after the transplantation of the donor uterine tissue. All twelve mice were euthanized for analysis 24 h after the last administration.

Measurement and histological analysis of murine endometriotic lesions

Identified endometriotic lesions were excised as single masses. The number of lesions were recorded, and the diameter of each lesion was measured. Lesion volume was calculated by measuring the width (α), length (β), and height (γ) and applying the formula for the volume of an ellipse ($V = 4/3 \pi abc$ [mm³]; $a = 1/2\alpha$, $b = 1/2\beta$, $c = 1/2\gamma$) as previously described [19].

The endometriotic lesions were fixed with 10% formalin solution for 24 h, replaced with 70% ethanol, embedded in paraffin, cut into sections of 3 μ m thickness, and examined by immunohistochemical analysis. Immunohistochemical staining was performed using a Leica Bond Max automated system (Leica, Bannockburn, IL, USA) according to the manufacturer's instruction. Primary antibodies were Ki67 (ab9260, 1:500, Abcam, Cambridge, UK), IL-6 (bs-0782R, 1:200, Bioss Antibodies, Woburn, MA, USA), PAX8 (ab97477, 1:2000, Abcam, Cambridge, UK), and PgR (ab16661, Abcam, Cambridge, UK) diluted to appropriate concentrations using BOND Primary Antibody Diluent (AR9352). Immunostaining was performed with either BOND Epitope Retrieval Solution 1 (AR9961) or 2 (AR9640), depending on the primary antibody used. AR9961 was used for anti-Ki67 antibody, anti-IL-6 antibody and anti-PgR antibody. AR9640 was used for anti-PAX8 antibody. The stained sections were observed under a microscope (Axio Imager 2, Zeiss, Oberkochen, Germany). Staining intensity was quantified using ImageJ software (threshold Ki67/180, Masson trichrome/200, IL-6/180).

Statistical analyses

Statistical analyses were performed using Student's *t*-tests or one-way analyses of variance (ANOVA) using Microsoft Excel and Prism 8 software (GraphPad, San Diego, CA, USA). The significance of the difference (*P* value) was calculated and defined as either * $P < 0.05$, ** $P < 0.01$, *** $P < 0.001$, or no significance (n.s.). Data are reported as means \pm standard error of the mean (SEM), unless specified otherwise.

Results

CSCs display characteristics of cellular senescence

To determine whether cellular senescence is involved in ovarian endometriosis, we assessed the prevalence of cellular senescence characteristics in nESCs, eESCs, and CSCs. We first analyzed senescence-specific morphological features (nuclear swelling and cytoplasmic expansion). These morphological features were more pronounced in CSCs than in nESCs or eESCs (nucleus: nESCs; $36.5 \pm 2.0 \mu\text{m}^2$, eESCs; $35.5 \pm 2.6 \mu\text{m}^2$, CSCs; $52.9 \pm 1.9 \mu\text{m}^2$, $P < 0.001$, cytoplasm: nESCs; $3415.8 \pm 33.5 \mu\text{m}^2$, eESCs; $2574.7 \pm 183.5 \mu\text{m}^2$, CSCs; $12181.8 \pm 2684.5 \mu\text{m}^2$, $P < 0.01$) (Fig. 2A–D). We next investigated SA- β -Gal

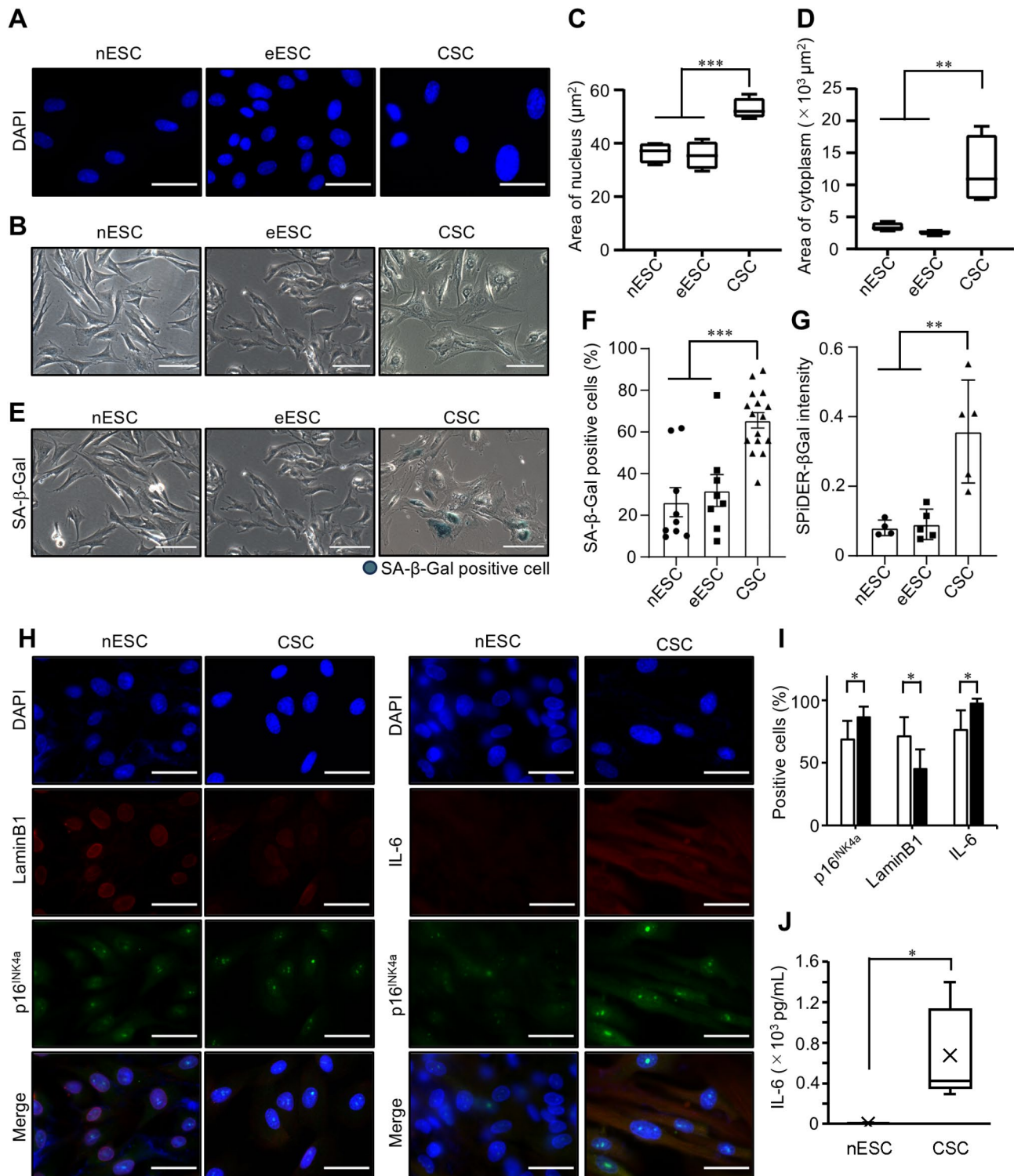


Fig. 2 (See legend on next page.)

expression via SA-β-Gal staining and fluorescent staining with the high-cell-permeant SPiDER-βGal. The proportion of SA-β-Gal staining positive cells in CSCs was significantly higher than that in nESCs or eESCs (nESCs: $26.3 \pm 7.0\%$, eESCs: $31.9 \pm 7.6\%$, CSCs: $65.6 \pm 3.7\%$,

$P < 0.001$) (Fig. 2E and F). SPiDER-βGal fluorescence, which quantifies SA-β-Gal activity, was elevated in CSCs compared to those in nESCs or eESCs (nESCs; 0.081 ± 0.011 , eESCs; 0.091 ± 0.020 , CSCs; 0.36 ± 0.066 , $P < 0.01$) (Fig. 2G). Finally, we evaluated the other

(See figure on previous page.)

Fig. 2 CSCs display characteristics of cellular senescence. **(A)** Representative images of nuclear swelling. Scale bar: 20 μ m. **(B)** Representative images of cytoplasmic expansion. Scale bar: 200 μ m. **(C)** The results of nuclear area quantitative analyses are shown in a box plot ($n=5$ in each group). **(D)** The results of cytoplasmic area quantitative analyses are shown in a box plot ($n=5$ in each group). **(E)** Representative SA- β -Gal staining images. Scale bar: 200 μ m. **(F)** The proportion of SA- β -Gal staining positive cells in each group is shown (nESCs; $n=9$, eESCs; $n=8$, CSCs; $n=16$). **(G)** Quantitation of SPIDER- β -Gal intensity is shown ($n=5$ in each group). **(H)** Representative immunocytochemistry images of senescence markers; p16^{INK4a}, laminB1, and IL-6. Scale bar: 20 μ m. Quantitative analysis is shown in **(I)** ($n=5$ in each group). **(J)** Supernatant IL-6 concentration is shown in the box plot ($n=5$ in each group). nESCs, normal endometrial stromal cells; eESCs, endometrial stromal cells with ovarian endometriosis (OE); CSCs, OE (chocolate cyst)-derived stromal cells; SA- β -Gal, senescence-associated β -galactosidase. **(C, D and J)** Horizontal lines centered within the boxes indicate median values. The bottom and top of the box indicate the 25th and 75th percentiles, respectively. The whisker ends indicate the respective minimum and maximum for all data. **(F, G and I)** Data are shown as means \pm SEM. Data were analyzed by a one-way ANOVA (**F** and **G**) and the Student's *t*-test (**I**). * $P < 0.05$; ** $P < 0.01$; *** $P < 0.001$; n.s., not significant

senescence markers, p16^{INK4a}, LaminB1, and IL-6, using immunocytochemistry. Proportions of p16^{INK4a} and IL-6 positive cells were higher and LaminB1 positive cells were lower in CSCs compared to those in nESCs (p16^{INK4a}: nESCs; $68.9 \pm 14.8\%$, CSCs; $87.0 \pm 8.2\%$, $P < 0.05$, IL-6: nESCs; $76.5 \pm 15.5\%$, CSCs; $97.8 \pm 3.8\%$, $P < 0.01$, LaminB1: nESCs; $71.4 \pm 15.2\%$, CSCs; $45.2 \pm 15.6\%$, $P < 0.05$) (Fig. 2H and I). IL-6 supernatant concentrations were significantly higher in CSCs than in nESCs (nESCs; 3.2 ± 1.8 pg/mL, CSCs; 677.8 ± 203.6 pg/mL, $P < 0.05$) (Fig. 2J).

Effects of AZM and ABT263 on cell viability and IL-6 secretion in CSCs

To evaluate the effects of senolytic drugs, such as AZM and ABT263, we added these drugs to cultured nESCs, eESCs and CSCs. Treatment with 50 μ M AZM for 72 h specifically reduced the surviving fraction in CSCs compared to 0 μ M AZM treatment (nESCs: 0.89 ± 0.22 , $P = 0.42$, eESCs: 1.06 ± 0.17 , $P = 0.99$, CSCs: 0.37 ± 0.04 , $P < 0.001$) (Fig. 3A). Treatment with 1 μ M ABT263 for 24 h reduced the surviving fraction in CSCs compared to 0 μ M ABT263 treatment (nESCs: 0.62 ± 0.12 , $P = 0.11$, eESCs: 0.36 ± 0.20 , $P = 0.20$, CSCs: 0.31 ± 0.08 , $P < 0.01$) (Fig. 3B). Although the difference was insignificant, ABT263 reduced the surviving fraction of nESCs and eESCs, whereas AZM had minimal effects on nESCs and eESCs (Fig. 3A and B). The number of SA- β -Gal positive cells decreased by approximately half after treatment with AZM or ABT263 (nESC: AZM, 0.47 ± 0.04 , $P < 0.001$, ABT263, 0.43 ± 0.08 , $P < 0.001$, CSC: AZM, 0.45 ± 0.07 , $P < 0.001$, ABT263, 0.48 ± 0.06 , $P < 0.001$) (Fig. S1A and B).

To evaluate SASP factors in nESCs and CSCs, we performed a cytokine array with the respective culture supernatants. Representative images of the cytokine array are shown in Fig. 3C. The integrated densities of IL-6, CXC motif ligand 1 (CXCL1), GRO a/b/g, and Interleukin-8 (IL-8) were significantly higher in CSCs than in nESCs (IL-6; $P < 0.0001$; CXCL1; $P < 0.001$; GRO a/b/g, $P < 0.05$; and IL-8; $P < 0.05$). Among these cytokines, IL-6 levels were significantly reduced by AZM treatment ($P = 0.056$) (Fig. 3C). The relative supernatant concentration of IL-6 was significantly reduced in CSCs

compared to that in nESCs with AZM treatment (nESCs: 0.69 ± 0.10 , CSCs: 0.36 ± 0.078 , $P < 0.05$) (Fig. 3D). By contrast, ABT263 did not impact the relative supernatant concentration of IL-6 (nESCs: 0.37 ± 0.095 , CSCs: 0.59 ± 0.14 , $P = 0.24$) (Fig. 3E).

AZM prevents endometriosis progression in murine models

The experimental protocol using our murine model is shown in Fig. 1A. AZM-treated and vehicle groups were euthanized 8 weeks after transplantation (at 17-week-old), and endometriotic lesions were evaluated. Multiple cystic lesions were observed in the abdominal cavity (Fig. S2A). The number of cysts was comparable between the vehicle- and AZM-treated groups (Fig. 1B and C). However, treatment with AZM for 4 weeks significantly reduced the volume per cyst compared to that in the vehicle group (81.9 ± 9.7 vs. 66.2 ± 18.5 mm³, $P < 0.05$) (Fig. 1B and D). Histological analysis of endometriotic lesions was performed by identifying the epithelial component via the pair-box (PAX) 8 expression [29] and the stromal component via progesterone receptor (PgR) expression (Fig. S2B). To evaluate proliferative activity within endometriotic lesions, the percentage of Ki67-positive cells was calculated. The percentage of Ki67-positive cells in endometriotic lesions decreased significantly in both epithelial and stromal cells (epithelial; 21.9 ± 8.2 vs. $7.4 \pm 4.6\%$, $P < 0.01$, stromal; 3.2 ± 0.9 vs. $0.7 \pm 0.3\%$, $P < 0.01$) after AZM treatment (Fig. 1E and F), and fibrotic lesions in endometriotic cysts were significantly reduced after AZM treatment (36.9 ± 2.8 vs. $13.7 \pm 2.6\%$, $P < 0.0001$) (Fig. 1G and H). We evaluated the effects of AZM on IL-6 expression in murine endometriotic cysts. IL-6-positive areas in epithelial cells were comparable with or without treatment, while in stromal cells, IL-6-positive areas significantly decreased after AZM treatment (epithelial; $30.4 \pm 2.2\%$ vs. $28.7 \pm 3.4\%$, $P = 0.66$, stromal; $20.0 \pm 2.1\%$ vs. $3.3 \pm 0.8\%$, $P < 0.0001$) (Fig. 1I and J). No mice died during the experiment. They were able to take standard amounts of chow and water, and normal feces were observed.

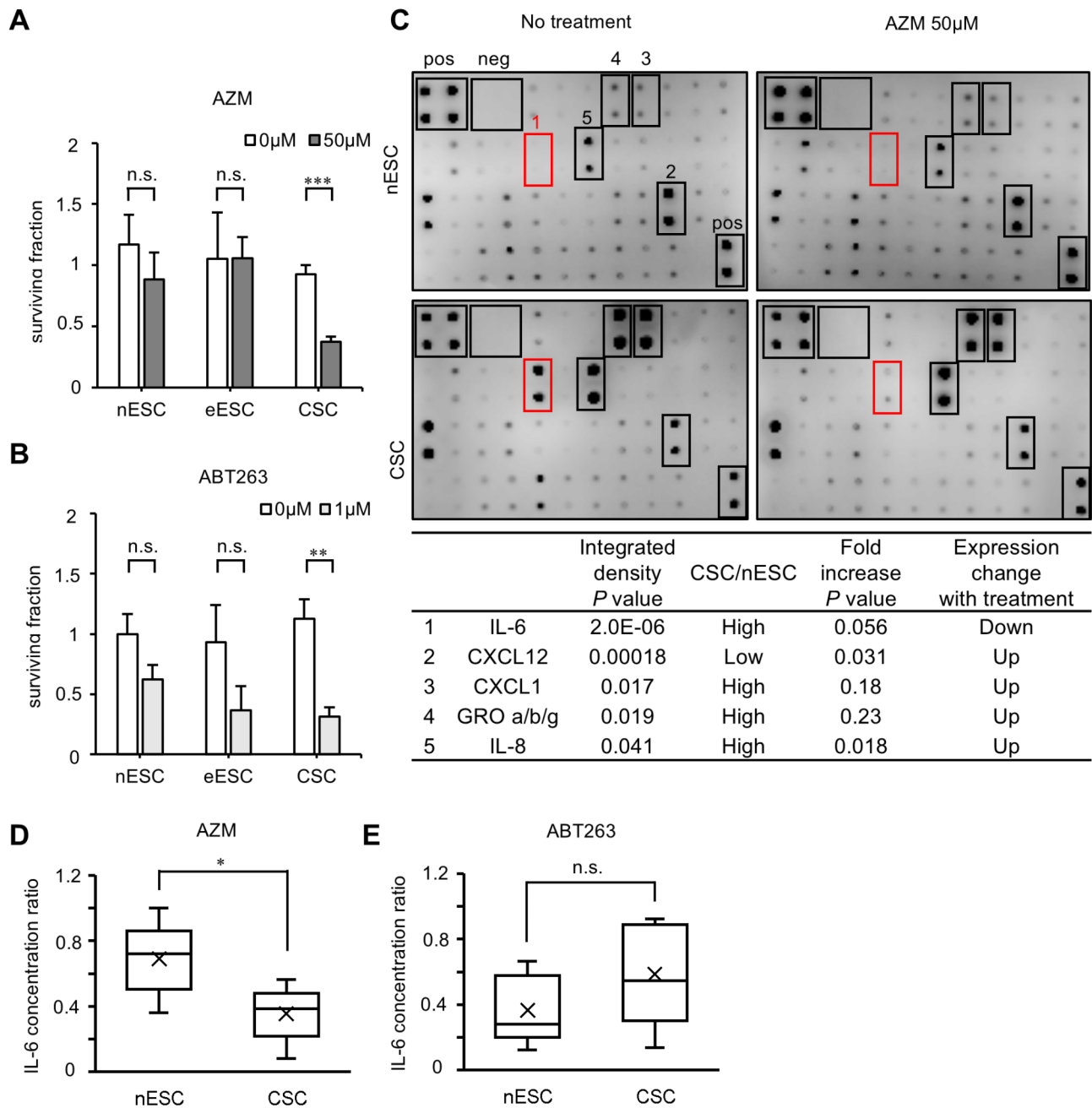


Fig. 3 Effects of AZM and ABT263 on cell viability and IL-6 secretion in CSCs. **(A)** AZM treatment reduces the viable cell fraction in CSCs ($n=5$ in each group). **(B)** ABT263 treatment reduces the viable cell fraction in CSCs ($n=5$ in each group). **(C)** Representative cytokine array ($n=4$ in each group) images (upper panels), quantification of intensity of each spot (middle table). **(D)** The ratio of supernatant IL-6 concentrations before vs. after AZM treatment is shown in box plot form ($n=5$ in each group). **(E)** The ratio of IL-6 concentrations before vs. after AZM treatment is shown in box plot form ($n=5$ in each group). nESCs, normal endometrial stromal cells; eESCs, endometrial stromal cells with ovarian endometriosis (OE); CSCs, OE (chocolate cyst)-derived stromal cells; AZM, azithromycin; ABT263, navitoclax. (A and B) Data are shown as means \pm SEM. (D and E) The horizontal line centered inside each box indicates the median. The bottom and top of the box indicate the 25th and 75th percentiles, respectively. The ends of the whiskers indicate the minimum and maximum of all the data. Data were analyzed by the Student's *t* test. * $P < 0.05$; ** $P < 0.01$; n.s., not significant

Discussion

Our study showed that CSCs contain more senescent cells compared to nESCs or eESCs. CSCs secreted IL-6 at the highest levels among other SASP factors examined. AZM and ABT263 reduced cell viability and AZM

effectively reduced IL-6 secretion in CSCs. Furthermore, AZM suppressed IL-6 expression and inhibited endometriosis progression in a murine model. To our knowledge, this is the first report to suggest that AZM may inhibit endometriosis progression.

The involvement of cellular senescence in endometriosis has recently been reported [21–24]. Our findings are in line with previous reports in that we observed an increase in several senescence markers expressions in endometriosis. While senotherapy for cancer and chronic inflammatory diseases have been actively investigated [3, 10, 11], no reports currently describe its efficacy in treating endometriosis. We thus assessed two senotherapeutics, the BCL-2 protein inhibitor ABT263, and the antibiotic AZM, which are known to exert highly specific cytotoxicity toward senescent fibroblasts [25, 26]. Although a clinical trial of ABT263 was conducted for cancer treatment in combination with anticancer agents, the trial was terminated due to its strong side effects such as grade 3 or 4 thrombocytopenia, and lymphocytopenia, increased in aminotransferases [30]. AZM is a frequently used antibiotic in obstetrics and gynecology with mostly tolerable side effects (including diarrhea) [31]. In this study, ABT263 induced cell death in nESC, eESC and CSC, while AZM specifically reduced cell viability in CSC, with less effects on nESC and eESC. Furthermore, although ABT263 was not effective, AZM inhibited IL-6 secretion in CSCs. Considering the side effects of ABT263 and the CSC-specific effects of AZM, AZM was selected for an in vivo study with a murine model. AZM reduced endometriotic lesion volume, epithelial and stromal proliferation, fibrotic lesions, and IL-6 expression. Our results suggest that AZM is a potential non-hormonal therapeutic for endometriosis via suppressing IL-6 expression.

Chronic inflammation is a key characteristic of endometriosis [1, 12]. However, the pathogenesis of chronic inflammation in endometriosis remains unclear. We hypothesized that cellular senescence might be a contributing factor of chronic inflammation, and we especially focused on SASP, a phenomenon in which senescent cells secrete bioactive substances, including cytokines. CSCs secreted IL-6 at the highest levels relative to all examined SASP factors, including IL-8, CXCL1, and GRO a/b/g. IL-6 is a multifunctional inflammatory cytokine produced by immune cells and fibroblasts [18]. Reports have associated it with increased ascites and serum levels in patients with endometriosis [13], suppression of early embryonic development, and reproductive disorders, including decreased sperm motility and suppression of estrogen production by granulosa cells [15, 16]. IL-8 promotes endometrial cell adhesion during endometriosis [32] and is associated with endometriotic infertility, as is IL-6 [17]. Chemokines such as CXCL1 have been implicated in the etiology of endometriosis [33, 34] and are commonly reported to be involved in fibrosis [35]. The senescent cells in endometriosis may be responsible for the increased secretion of these inflammatory factors via SASP.

In turn, senescent cells in endometriosis may arise from the high oxidative stress levels associated with endometriosis. High levels of oxidative stress contribute to the excessive endometrial cell proliferation, characteristic of endometriosis, as well as inflammation and angiogenesis [20, 36]. Oxidative stress may cause SIPS, leading to the formation of senescent cells, although further investigation is required for confirmation.

This study has some limitations. First, we did not investigate each specific menstrual phase. Cellular senescence is involved in endometrial dedifferentiation [37]; IL-6 expression is low during the proliferative phase and high during the secretory and menstrual phases [38]. In this study, we observed that the proportion of senescent cells varied among patients with endometriosis. We believe there is room for further investigation of these factors (age, disease history, course, etc.) in patients with a high fraction of senescent cells who experience different treatment efficacies. Second, it is yet unclear whether the presented AZM inhibitory effects on endometriosis are not due to its antimicrobial effects, but solely due to its senotherapeutic effects. Metronidazole has been reported to reduce endometriosis progression in mice [39]; Antibiotic treatment targeting *Fusobacterium* in the endometrium has been reported as a therapeutic option for patients with endometriosis [40]. The current study did not examine the antimicrobial effects of AZM in endometriosis. Finally, the effects of AZM on ovarian functions, including follicle development, oocyte quality, and fertility were not evaluated due to the use of a peritoneal endometriosis mouse model in this study [28]. Further investigation in an OE mouse model is required to fully evaluate the effects of AZM on ovarian function [41].

Conclusions

Cellular senescence is involved in the pathogenesis of endometriosis and AZM may be useful for preventing endometriosis progression by suppressing IL-6 secretion of a SASP. This study shows that AZM may serve as a potential non-hormonal therapeutic treatment for endometriosis. A new focus on cellular senescence may reveal novel therapeutic approaches for endometriosis.

Abbreviations

ABT263	Navitoclax
ANOVA	Analyses of variance
AZM	Azithromycin
BCL-2	B-cell lymphoma-2
CLEIA	Chemiluminescent enzyme immunoassay
CSCs	OE cyst-derived stromal cells
CXCL1	CXC motif ligand 1
eESCs	Endometrial stromal cells with endometriosis
IL-6	Interleukin-6
IL-8	Interleukin-8
nESCs	Normal endometrial stromal cells
NLRP	Nucleotide-binding oligomerization domain, leucine-rich repeat, and pyrin domain
OE	Ovarian endometriosis

OS	Oxidative stress
p16 ^{INK4a}	Cyclin-dependent kinase inhibitor 2 A locus
PAX	Pair-box
PBS	Phosphate-buffered saline
PgR	Progesterone receptor
SA-b-Gal	Senescence-associated b-galactosidase
SASP	Senescence-associated secretory phenotype
SEM	Standard error of the mean
SIPS	Stress-induced premature senescence
X-Gal	5-bromo-4-chloro-3-indolyl-β-D-thiogalactopyranoside

Supplementary Information

The online version contains supplementary material available at <https://doi.org/10.1186/s12958-025-01381-4>.

Supplementary Material 1

Supplementary Material 2

Acknowledgements

The authors thank Bayasula M.D., Ph.D. (Bell Research Center for Reproductive Health and Cancer, Nagoya University Graduate School of Medicine, Nagoya, Aichi, Japan) for providing excellent technical assistance.

Author contributions

RS, TN and HK conceived and designed this study. RS, SK, HT and AM collected and analyzed the data. RS, TN, TT, TS, AY, NM, SO, AI and HK. interpreted the whole results. RS and TN wrote the manuscript. All authors reviewed the manuscript.

Funding

This work was supported by the Grant-in-Aid for Scientific Research 23K08820 to Tomoko Nakamura from the Japan Society for the Promotion of Science, Japan.

Data availability

No datasets were generated or analysed during the current study.

Declarations

Ethics approval and consent to participate

The ethics committee of the Nagoya University Graduate School of Medicine (2017–0503) approved the experiments. Written informed consent as obtained from each patient prior to participation in the study. All animal experiments were approved by the Animal Experimental Committee of the Nagoya University Graduate School of Medicine (M230117-002 and M230297-002).

Consent for publication

Not applicable.

Competing interests

The authors declare no competing interests.

Author details

¹Department of Obstetrics and Gynecology, Nagoya University Graduate School of Medicine, 65 Tsurumai-chou, Showa-ku, Nagoya 466-8550, Aichi, Japan

²Department of Maternal and Perinatal Medicine, Nagoya University Hospital, 65 Tsurumai-chou, Showa-ku, Nagoya 466-8550, Aichi, Japan

³Department of Obstetrics and Gynecology, Gunma University Graduate School of Medicine, 3-39-22 Showa-machi, Maebashi 371-8511, Gunma, Japan

Received: 5 September 2024 / Accepted: 10 March 2025

Published online: 26 March 2025

References

1. Becker CM, Bokor A, Heikinheimo O, Horne A, Jansen F, Kiesel L et al. ESHRE guideline: endometriosis. *Hum Reprod Open*. 2022;2022:hoac009.
2. He S, Sharpless NE. Senescence in health and disease. *Cell*. 2017;169:1000–11.
3. Lozano-Torres B, Estepa-Fernández A, Rovira M, Orzáez M, Serrano M, Martínez-Mañez R, et al. The chemistry of senescence. *Nat Reviews Chem*. 2019;3:426–41.
4. Lopes-Paciencia S, Saint-Germain E, Rowell MC, Ruiz AF, Kalegari P, Ferbeyre G. The senescence-associated secretory phenotype and its regulation. *Cytokine*. 2019;117:15–22.
5. de Magalhães JP, Passos JF. Stress, cell senescence and organismal ageing. *Mech Ageing Dev*. 2018;170:2–9.
6. McHugh D, Gil J. Senescence and aging: causes, consequences, and therapeutic avenues. *J Cell Biol*. 2018;217:65–77.
7. Acosta JC, O’Loughlin A, Banito A, Guijarro MV, Augert A, Raguz S, et al. Chemokine signaling via the CXCR2 receptor reinforces senescence. *Cell*. 2008;133:1006–18.
8. Kulman T, Michaloglou C, Vredeveld LC, Douma S, van Doorn R, Desmet CJ, et al. Oncogene-induced senescence relayed by an interleukin-dependent inflammatory network. *Cell*. 2008;133:1019–31.
9. Mehdizadeh M, Aguilar M, Thorin E, Ferbeyre G, Nattel S. The role of cellular senescence in cardiac disease: basic biology and clinical relevance. *Nat Rev Cardiol*. 2022;19:250–64.
10. Ngoi NY, Liew AQ, Chong SJF, Davids MS, Clement MV, Pervaiz S. The redox-senescence axis and its therapeutic targeting. *Redox Biol*. 2021;45:102032.
11. Chaib S, Tchkonja T, Kirkland JL. Cellular senescence and senolytics: the path to the clinic. *Nat Med*. 2022;28:1556–68.
12. Scutiero G, Iannone P, Bernardi G, Bonaccorsi G, Spadaro S, Volta CA et al. Oxidative stress and endometriosis: a systematic review of the literature. *Oxid Med Cell Longev*. 2017;2017:7265238.
13. Harada T, Yoshioka H, Yoshida S, Iwabe T, Onohara Y, Tanikawa M, et al. Increased interleukin-6 levels in peritoneal fluid of infertile patients with active endometriosis. *Am J Obstet Gynecol*. 1997;176:593–7.
14. Ganieva U, Nakamura T, Osuka S, Bayasula, Nakanishi N, Kasahara Y, et al. Involvement of transcription factor 21 in the pathogenesis of fibrosis in endometriosis. *Am J Pathol*. 2020;190:145–57.
15. D’Hooghe TM, Xiao L, Hill JA. Cytokine profiles in autologous peritoneal fluid and peripheral blood of women with deep and superficial endometriosis. *Arch Gynecol Obstet*. 2001;265:40–4.
16. Taskin MI, Gungor AC, Adali E, Yay A, Onder GO, Inceboz U. A humanized anti-interleukin 6 receptor monoclonal antibody, tocilizumab, for the treatment of endometriosis in a rat model. *Reprod Sci*. 2016;23:662–9.
17. Malvezzi H, Hernandez C, Piccinato CA, Podgaec S. Interleukin in endometriosis-associated infertility-pelvic pain: systematic review and meta-analysis. *Reproduction*. 2019;158:1–12.
18. Symons LK, Miller JE, Kay VR, Marks RM, Liblik K, Koti M, et al. The immunopathophysiology of endometriosis. *Trends Mol Med*. 2018;24:748–62.
19. Murakami M, Osuka S, Muraoka A, Hayashi S, Bayasula, Kasahara Y, et al. Effectiveness of NLRP3 inhibitor as a non-hormonal treatment for ovarian endometriosis. *Reprod Biol Endocrinol*. 2022;20:58.
20. Clower L, Fleshman T, Geldenhuys WJ, Santanam N. Targeting oxidative stress involved in endometriosis and its pain. *Biomolecules*. 2022;12.
21. Malvezzi H, Viana BG, Dobo C, Filippi RZ, Podgaec S, Piccinato CA. Depleted lamin B1: a possible marker of the involvement of senescence in endometriosis? *Arch Gynecol Obstet*. 2018;297:977–84.
22. Malvezzi H, Cestari BA, Meola J, Podgaec S. Higher oxidative stress in endometriotic lesions upregulates senescence-associated p16(ink4a) and beta-galactosidase in stromal cells. *Int J Mol Sci*. 2023;24.
23. Malvezzi H, Dobo C, Filippi RZ, Mendes do Nascimento H, Palmieri da Silva ESL, Meola J et al. Altered p16(ink4a), IL-1beta, and lamin b1 protein expression suggest cellular senescence in deep endometriotic lesions. *Int J Mol Sci*. 2022;23.
24. Palmieri L, Malvezzi H, Cestari B, Podgaec S. Colocalization of senescent biomarkers in deep, superficial, and ovarian endometriotic lesions: a pilot study. *Sci Rep*. 2022;12:17280.
25. Ozsvari B, Nuttall JR, Sotgia F, Lisanti MP. Azithromycin and roxithromycin define a new family of senolytic drugs that target senescent human fibroblasts. *Aging-Us*. 2018;10:3294–307.
26. Chang J, Wang Y, Shao L, Laberge RM, Demaria M, Campisi J, et al. Clearance of senescent cells by ABT263 rejuvenates aged hematopoietic stem cells in mice. *Nat Med*. 2016;22:78–83.

27. Masaldan S, Clatworthy SAS, Gamell C, Meggyesy PM, Rigopoulos AT, Haupt S, et al. Iron accumulation in senescent cells is coupled with impaired ferritinophagy and inhibition of ferroptosis. *Redox Biol.* 2018;14:100–15.
28. Ishida C, Mori M, Nakamura K, Tanaka H, Mizuno M, Hori M, et al. Non-thermal plasma prevents progression of endometriosis in mice. *Free Radic Res.* 2016;50:1131–9.
29. Arakawa T, Fukuda S, Hirata T, Neriishi K, Wang Y, Takeuchi A, et al. PAX8: a highly sensitive marker for the glands in extragenital endometriosis. *Reprod Sci.* 2020;27:1580–6.
30. Wilson WH, O'Connor OA, Czuczman MS, LaCasce AS, Gerecitano JF, Leonard JP, et al. Navitoclax, a targeted high-affinity inhibitor of BCL-2, in lymphoid malignancies: a phase 1 dose-escalation study of safety, pharmacokinetics, pharmacodynamics, and antitumour activity. *Lancet Oncol.* 2010;11:1149–59.
31. Jensen JS, Cusini M, Gomberg M, Moi H, Wilson J, Unemo M. 2021 European guideline on the management of Mycoplasma genitalium infections. *J Eur Acad Dermatol Venereol.* 2022;36:641–50.
32. Sikora J, Smycz-Kubanska M, Mielczarek-Palacz A, Kondera-Anasz Z. Abnormal peritoneal regulation of chemokine activation-the role of IL-8 in pathogenesis of endometriosis. *Am J Reprod Immunol.* 2017;77.
33. Nishida M, Nasu K, Narahara H. Role of chemokines in the pathogenesis of endometriosis. *Front Biosci (Schol Ed).* 2011;3:1196–204.
34. Zhu R, Nasu K, Aoyagi Y, Hirakawa T, Takebayashi K, Narahara H. Chemokine expression profiles of ovarian endometriotic stromal cells in three-dimensional culture. *J Reprod Immunol.* 2020;138:103100.
35. Barnes PJ, Baker J, Donnelly LE. Cellular senescence as a mechanism and target in chronic lung diseases. *Am J Respir Crit Care Med.* 2019;200:556–64.
36. Al-Hetty H, Jabbar AD, Eremin VF, Jabbar AM, Jalil AT, Al-Dulimi AG, et al. The role of endoplasmic reticulum stress in endometriosis. *Cell Stress Chaperones.* 2023;28:145–50.
37. Deryabin P, Griukova A, Nikolsky N, Borodkina A. The link between endometrial stromal cell senescence and decidualization in female fertility: the art of balance. *Cell Mol Life Sci.* 2020;77:1357–70.
38. Korbecki J, Szatkowska I, Kupnicka P, Żwieręto W, Barczak K, Poziomkowska-Gęsicka I et al. The importance of CXCL1 in the physiological state and in noncancer diseases of the oral cavity and abdominal organs. *Int J Mol Sci.* 2022;23.
39. Chadchan SB, Cheng M, Parnell LA, Yin Y, Schriefer A, Mysorekar IU, et al. Antibiotic therapy with metronidazole reduces endometriosis disease progression in mice: a potential role for gut microbiota. *Hum Reprod.* 2019;34:1106–16.
40. Muraoka A, Suzuki M, Hamaguchi T, Watanabe S, Iijima K, Murofushi Y, et al. Fusobacterium infection facilitates the development of endometriosis through the phenotypic transition of endometrial fibroblasts. *Sci Transl Med.* 2023;15:eadd1531.
41. Hayashi S, Nakamura T, Motooka Y, Ito F, Jiang L, Akatsuka S, et al. Novel ovarian endometriosis model causes infertility via iron-mediated oxidative stress in mice. *Redox Biol.* 2020;37:101726.

Publisher's note

Springer Nature remains neutral with regard to jurisdictional claims in published maps and institutional affiliations.